Optica Applicata, Vol. XXII, No. 3–4, 1992

XeCl theoretical model for computer controlled excimer laser

L. POKORA, Z. UJDA

Institute of Quantum Electronics, ul. S. Kaliskiego 6, 01–489 Warszawa, Poland.

The theoretical model and computing results of XeCl laser output parameters are presented. Multilevel model of radiation extraction was worked out, including all important processes which have significant influence on laser output. Presented results concern both construction and laser input parameters which can be automatically controlled. In particularly, the gas pressure, percentage gas composition and charging voltage depending on laser output parameters such as laser energy, peak power, pulse width and efficiency were studied. Obtained results allow microprocessor control of excimer laser in a wide range.

1. Introduction

Computerization and automation of many research and experimental works affect also the design of lasers, permitting their microprocessor control. Computer control is required especially for multi-component gas lasers, including the excimer lasers. Besides the very attractive properties of generated radiation, they are characterized by high complexity of internal processes [1], [2] and sensitivity to many external parameters [3]. This makes automation more difficult [4] and complicates the theoretical model required to implement the controlling algorithm [5].

This discussion will concentrate upon the XeCl laser (He:Xe:HCl) pumped by an electric discharge with automatic preionization by UV radiation. The model presented below is intended to be a comprehensive one, *i.e.* it covers all important groups of problems leading together to the output characteristics of the laser. The model permits the microprocessor controlling of the output parameters by altering supply voltage, pressure and percentage composition of the gas mixture.

2. Description of the theoretical model

The analysis of the excimer laser presented in this paper has been made for an L–C inverted electric circuit, as presented in Fig. 1. The preionization circuit is an integrated part of the main circuit. The initiation of laser operation takes place through a commuting element.

The model assumes a time-varying value of resistance in both the commutator I and in the preionization elements P. The resistance in those elements has been calculated from the following formula:

$$\frac{dR_{I,P}}{dt} = -\frac{R_{I,P}^2 I_I^{2/3}}{C_B d_{I,P} g_{I,P}^{1/3}}(n_P) \tag{1}$$

where: d – distance between discharge electrodes,
g – density of the working gas,
C_B – experimental constant [6],
n_P – number of preionization needle electrodes.

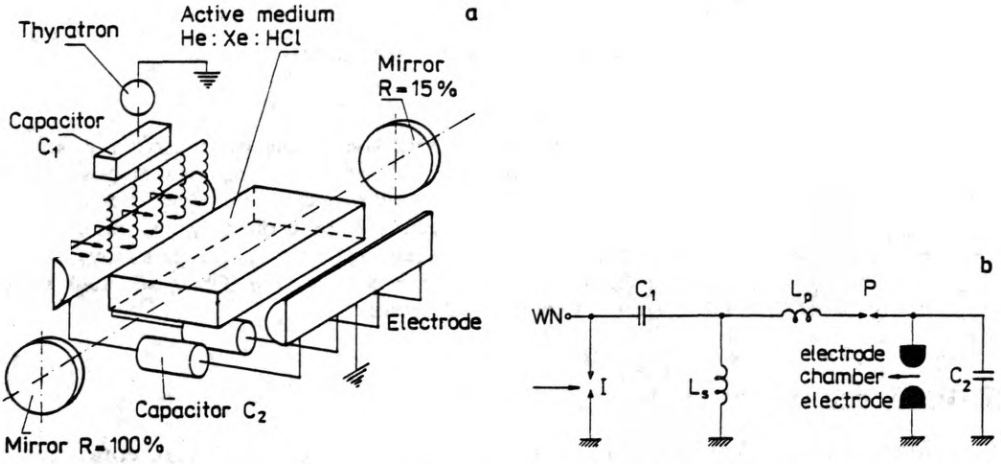

Fig. 1. Scheme of the excimer laser pumped with an electric discharge (a) and scheme of an electric circuit of an excimer laser adopted for theoretical analysis (b). I – commutator, P – preionization spark gaps, C_1 – storage capacitors battery, C_2 – discharge capacitors battery, L_s – separating coils, L_p – inductiveness of the spark gap leads

Description of the main discharge in the laser chamber has been characterized by the differential equation taken from [1]

$$\frac{dR_K}{dt} = -\frac{A_K}{d_K} R_K^2 \left(\mu \frac{dN_E}{dt} + N_E \frac{d\mu}{d\varepsilon}\frac{d\varepsilon}{dt}\right), \tag{2}$$

where: d_K, A_K – distance and surface area of electrodes in the chamber, respectively,
e – electron charge,
μ – mobility of electrons,
N_E – concentration of electrons in the active medium.

The adoption of a differential equation permits the follow-up in rate of resistivity change relative to changes of the current flow. Assessment of the breakdown voltages in the chamber and for preionization is made depending on the composition of the gas mixture and its pressure. The system of ordinary differential equations describing the laser electric circuit is coupled with the equations describing kinetics of the active medium through the varying in time N_E and μ.

The analysis of energy transitions in a three-component, ionized quantum mechanics system of the XeCl laser has been made with several simplifying assumptions. For the needs of this model we have assumed:

- uniformity of the active medium during an electric discharge,
- distribution of electron velocity of Maxwell type,
- identity of the beam cross-section and discharge area,
- one-dimensional model for radiation extraction.

The Maxwell type distribution of electron velocity refers to the period of maximum electron concentration (about 10^{15} cm^{-3}). This is a period of rapid thermalization of electrons while the changes in particle concentration in the upper and lower laser state are slight. This is simultaneously a period in which over 90% of the laser energy is emitted [7].

The model accounts for all important reactions taking place in the He-Xe-HCl model (105 reactions). Kinetics of the medium considers the following atomic and particle states: He, He*($^3S_1$ and $^1S_0$), He^+, He_2^*, Xe*($^3P_2$), Xe**(p), Xe^+, Xe_2^* Xe_2^{**}, Xe_2^+, Xe_3^*, HCl ($v = 0$), HCl ($v = 1$), HCl ($v = 2$), Cl^-, XeCl*(B) (upper level), XeCl(X) (lower level), Xe_2Cl^*. Thus, the laser medium has been described using a 19 level system. This list is supplemented by the electrons and photons. A wider discussion of these problems has been given in paper [5].

This model proposes to analyse preionization by expanding the equations describing concentration and energy of electrons. The level of preionization and its contribution to kinetics of the medium has been related to the electric circuit. We assume that concentration of preionization electrons is proportional to electric power freed in the spark gaps. Electrons formed as a result of preionization have been considered in the general system of equations by adding the following expressions:

$$\left(\frac{dN_E}{dt}\right)_P = \frac{\eta P_P}{V_K \varepsilon_P}, \tag{3}$$

$$\left(\frac{d(\varepsilon N_E)}{dt}\right)_P = \frac{\eta P_P}{V_K} \tag{4}$$

where: P_P – electric power freed during preionization spark discharge,
V_K – volume of the laser chamber,
ε_P – average energy of electrons formed as a result of photoionization,
η – efficiency of formation of electrons having energy ε_P.

The rate of electron formation due to preionization in our model is of the 10^7 cm^3/ns range.

The model calculates the time characteristics of a radiation pulse by solving the equation for concentration of photons in the resonator. Power of radiation is calculated more accurately during the quasi-stationary phase, which considers two counter-current streams of photons in the resonator. It may be then assumed that radiating power is constant (similarly to the other parameters) over a period of time equal to twice the time of light passing through the resonator (about 4 ns).

The radiation extraction model [8] takes into account oscillatory relaxation in the B state and collision mixing of the B–C states. Description of the XeCl laser radiation extraction has been based upon the modified Rigrod model. The XeCl* molecules in states B and C are established at the rate $0.77R$ (B) and $0.23R$ (C),

where R is the rate of formation for all $XeCl^*$ molecules. Laser emission takes place from the lowest oscillation level $B(v = 0)$. This permits to separate the $B(v = 0)$ state from the other B states, where the $B(v = 0)$ is the upper laser state. Next, it was considered that $XeCl^*(B)$ molecules are established at high oscillation levels and attain the laser level $B(v = 0)$ as a result of oscillatory relaxation.

Finally, this model describes the XeCl molecules by a four level model, with B, $B(v = 0)$, C and X and a laser transition (308 nm) between $B(v = 0)$ and X. Consequently, the XeCl excimer laser model presented is described by a system of 30 ordinary differential equations and one implicit equation. Introduction of symbolic notation for the reactions made the program versatile, *i.e.*, applicable to any excimer laser.

3. Selected result of computer calculations

The selected series of numerical calculations presented below has been made for a fixed set of physical parameters of the laser. The following laser parameters were used in the calculations:

- capacity $C_1 = 100$ nF, $C_2 = 32$ nF (16×2 nF),
- inductances $L_I = 120$ nH, $L_P = 40$ nH (2.4 μH/60), $L_K = 5$ nH, $L_s = 4$ nH,
- parasitic resistances $R_{IP} = 0.8\ \Omega$, $R_{PP} = 0.1\ \Omega$,
- supply voltage 30 kV,
- effective dimensions of the chamber (discharge volume) $d_K = 2$ cm, $l_K = 50$ cm, $s_K = 1$ cm,
- length of resonator $l_R = 70$ cm,
- number of spark gaps in the preionization system — 60, spacing of preionization electrodes $d_P = 0.1$ cm,
- mirror reflectivity (for 308 nm) $R_1 = 0.15$, $R_2 = 0.99$,
- composition of gas mixture He:Xe:HCl = 92:7.5:0.5,
- total pressure of gas mixture $p = 2000$ hPa or $p = 3000$ hPa.

Total results obtained give a characteristic of the electric circuit, kinetics of the laser system efficiency of the radiation extraction. The results have been described in detail in paper [7]. Here, we present the influence of electrode spacing and inductiveness of the chamber on the output parameters of the laser.

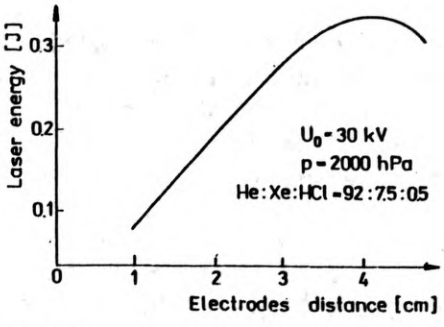

Fig. 2. Radiation energy as a function of electrode distance

Figure 2 presents dependence of the radiation energy upon the electrode spacing. For the electrode spacing under about 4 cm the increase in maximum power (electric pulse and radiation), and also energy evolved and radiated is almost linear in function of the electrode spacing.

The half-time of pulse duration is weakly dependent on the distance between electrodes. It changes from about 30 ns ($d_K = 1$ cm) to about 27 ns ($d_K = 4$ cm). While power of radiation reaches its maximum at electrode spacing of about 4.3 cm, intensity of radiation is maximum for $d_K = 3$ cm at about 3.5 MW/cm^2. Note that the power of radiation is not a linear function of electrode spacing. There are certain optimal electrode spacings (for power or power density of radiation), which are an outcome of many interdependences associated with its change. These include the effect upon the E/N parameter, electric resistivity and current in the chamber, cross-section of the radiation beam.

Inductance of the chamber L_K affects neither maximum voltge within the chamber, nor the voltage plateau (about 12 kV), but affects its duration. Figure 3 shows the change in time of laser radiation power for various L_K values. Pulse

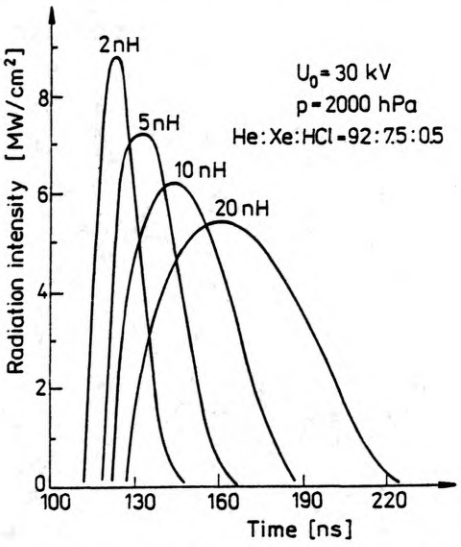

Fig. 3. Laser radiation power characteristics for various inductiveness of the chamber

characteristics of radiation are very similar to the corresponding current pulses (not shown here). Maximum power of radiation decreases with an increase in L_K, from some 9 MW for $L_K = 2$ nH to about 5.5 MW or $L_K = 20$ nH. Instead, the half-time of pulse duration extends considerably, from about 18 ns to 65 ns. Similarly, radiation energy increases from about 160 mJ to about 350 mJ, respectively.

Further work has been concentrated on presentation of the calculation results referring to the amount of laser radiation generated in a way depending on the external parameters, which could be computer controlled, *i.e.* charging voltage, pressure and composition of the gas. This group of calculations and analyses is

most important from the point of view of computerized control of the excimer laser operation.

One of the easier to implement parameters for controlling is the voltage U_0 which is used to charge to storage capacitor battery. Radiation energy dependence on U_0 is presented in Fig. 4. The radiated energy changes from about 100 mJ for $U_0 = 20$ kV to about 235 mJ at $U_0 = 40$ kV. This dependence is almost linear. Duration of the electric pulse changes slightly as a function of the charging voltage from about 32 ns for $U_0 = 20$ kV to about 25 ns at $U_0 = 40$ kV.

The above dependences for radiated energy (as well as total efficiency of the laser) are similar to those given in [9] for the XeCl(Ne) laser with similar construction.

The effect of total pressure p_0 of the working gas upon properties of the excimer laser is seen in the change in small signal amplification coefficient g_0 and coefficient for absorption laser radiation α, deciding about the amount of the generated laser radiation.

Maximum radiation laser energy is attained at about 200 mJ for $p_0 = 2300$ hPa as is shown in Fig. 5. With increase in pressure, duration of the radiation pulse and the electric pulse decreases. Duration of the radiation pulse changes from 28.5 ns to 22 ns.

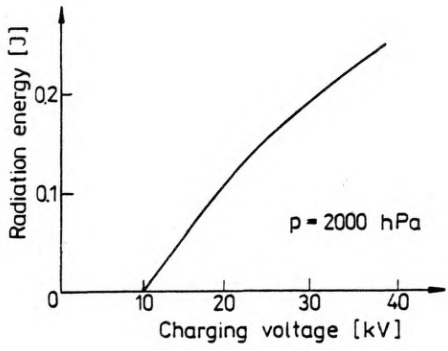

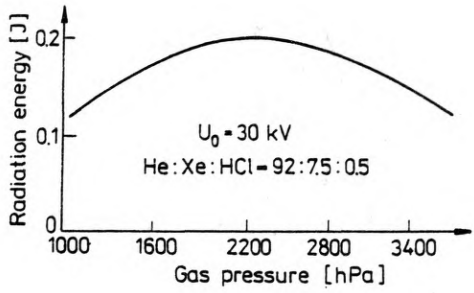

Fig. 4. Radiated energy as a function of the charging voltage

Fig. 5. Energy of the laser radiation as a function of the gas pressure

The computer control of the gas laser may take place also through changing the individual gas mixture components. In the case considered here, the laser is the most sensitive to the changes in Xe and HCl content. Figure 6 shows the dependence of laser radiation energy on content of Xe in the gas mixture. Both at $p_{HCl} = 10$ hPa and $p_{HCl} = 5$ hPa in the analysed range of Xe partial pressures the energy radiated has its maximum (at Xe content at 150–200 hPa) of about 200 mJ and 175 mJ, respectively.

Duration of the electric pulse shows a weak dependence on Xe content in the gas mixture and varies from 33 to 35 ns for HCl pressure equal to both 10 hPa and

5 HPa. The same is true for laser pulse duration, though that dependence is slightly stronger, especially at $p_{HCl} = 5$ hPa. This duration changes from 25 ns to 30 ns over the analysed range of Xe pressures. Note, however, that in the analysed range of Xe pressures, duration of the electric pulse increases slightly while duration of the radiation pulse decreases.

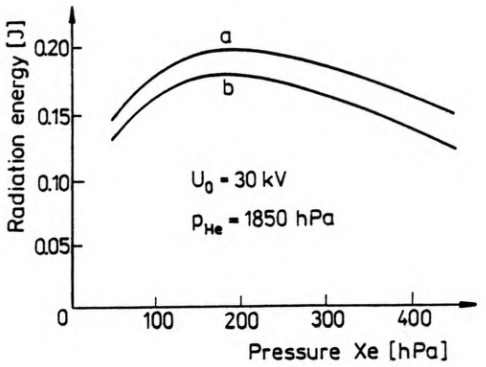

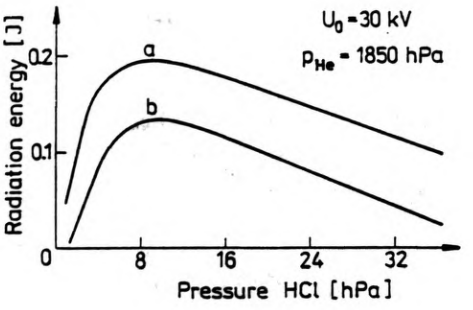

▲

Fig. 6. Radiation energy as a function of partial pressure of Xe for various pressures of HCl (a – p_{HCl} = 10 hPa, b – p_{HCl} = 5 hPa)

Fig. 7. Radiation energy as a function of HCl partial pressure for various partial pressures of Xe (a – p_{Xe} = 150 hPa, b – p_{Xe} = 500 hPa)

Figure 7 presents dependence of the radiated energy as a function of HCl content. The highest amount of radiated energy has been achieved for HCl content at about 10 hPa (about 0.5%) and this was independent of the Xe content; but at Xe 150 hPa the energy was higher at about 185 mJ, while at Xe 500 hPa it reached just about 400 mJ. This extremum in both cases was quite distinct.

The maximum efficiencies attainable at Xe pressures of 150 hPa and 500 hPa differ significantly from one another and have been reached for various HCl and Xe partial pressures (for total, internal and electric efficiencies, the optimal ratios of HCl and Xe partial pressure are 0.06, 0.03 and 0.14, respectively, at Xe 150 hPa, and 0.02, 0.02 and 0.02, respectively, at Xe 500 hPa).

Duration of the radiation pulse presented in Figure 8 is the highest for partial HCl pressure of about 5 hPa at Xe pressure 150 hPa (about 30 ns) and for HCl partial pressure 10 hPa at Xe 500 hPa (about 26 ns). At Xe 150 hPa the dependence of pulse duration is weaker than at Xe 500 hPa (*e.g.* at HCl 40 hPa duration of the laser pulse is 20 ns and 10 ns, respectively). The electric pulse is longer than the radiation pulse (maximum duration of about 35 ns) and again, its dependence on HCl content is weaker at Xe 150 hPa than at Xe 500 hPa.

The above results presenting the influence of HCl content on duration of the radiation pulse differ slightly from those contained in [10]. There, the received function was monotonous. The main difference is due to different methods applied to excite the laser medium. The laser presented in [10] was excited with an

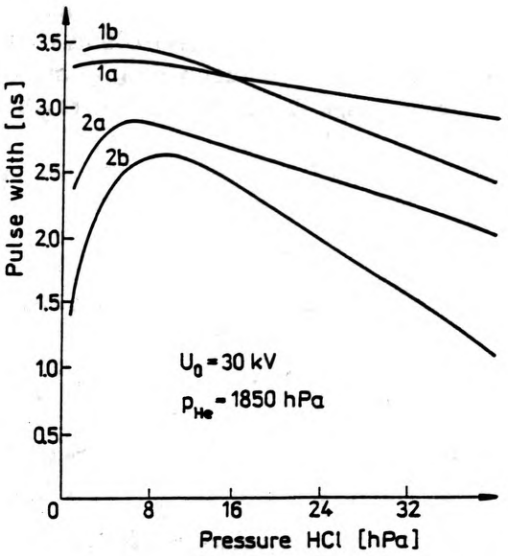

Fig. 8. Duration of laser radiation pulse and electrical pulse as a function of HCl partial pressures from various Xe partial pressures (a – $p_{Xe} = 150$ hPa, b – $p_{Xe} = 500$ hPa, 1 – electrical pulse, 2 – radiation pulse)

electric pulse (much longer than the radiation pulse), and it was then possible to discern the influence of HCl content on duration of the radiation pulse. Calculations presented in this work refer to the type of laser with a relatively short excitation pulse (comparable with duration of the radiation pulse). Thus, duration of the radiation pulse is considerably restricted by duration of the exciting pulse and the influence of HCl content on duration of the radiation pulse is in this case difficult to separate, more because content of HCl also affects directly shape of the electric pulse.

Both in the case of HCl as well as of Xe, the lines representing dependence of initial laser parameters on concentration have maxima, stronger in the first and weaker in the second case. This is associated with superimposing of two classes of processes: *i.e.*, those which lead to formation of the excimer and the influence of which increases with increasing concentration of the particles, and two, the quenching processes (collision damping) of the upper laser state and absorption of addition – also dependent upon pressure. The latter processes are, of course, the more important the higher HCl and Xe particles concentration. A stronger influence of HCl concentration on laser parameters may result from the contribution of HCl particles to dissociative adhesion of electrons leading to formation of the negative chloride ion, Cl^-. The formation of those ions strongly affects the course of kinetic reactions due to electron binding and, thus, affecting the discharge itself.

4. Extent of laser parameters control

The following external parameters are susceptible to control:

– charging voltage,

– total pressure of gas mixture,
– pressure of the halogen donor (HCl),
– pressure of noble gas (Xe),

There is also the possibility of controlling the other external parameters, *e.g.*, gas temperature, but an analysis has been reduced to the above parameters only, because they affect most strongly the operation of an excimer laser.

The output parameters, for which the data grid was developed were as follows:
– energy of the radiation pulse,
– peak power of the radiation pulse,
– half-time duration of the radiation pulse,
– total efficiency of the laser.

The relationships between the individual external and output parameters of the laser have already been discussed. At the adopted range of variability presented in Table 1, output parameters of the XeCl laser may be altered (selected) within a defined range, which has been presented in Table 2.

Table 1. Range of external parameters

Charging voltage	20–40 kV
HCl partial pressure	1–50 hPa
Xe partial pressure	50–500 hPa
He partial pressure	1850–3700 hPa

When setting values of one or few output parameters of the XeCl laser, as presented in Tab. 2, the data grid permits to select points which give a result close to the desired value in the following system of coordinates: charging voltage, values of partial pressures HCl, Xe and He. Next, the due approximation is made (usually linear, but also curvilinear when higher accuracy is required).

Table 2. Range of output parameters variability

Energy of the radiation pulse	0–330 mJ
Peak power of the radiation pulse	0–11 MW
Half-time duration of the radiation pulse	8–32 ns
Total efficiency of the laser	0–0.5%

Selection of the irradiated energy takes place first by determining the charging voltage (around middle of the range) as this gives the highest possibility to alter the radiated pulse energy, with partial pressures of the gas components selected next. In the case of selecting the duration time, first partial pressures are determined, beginning with the HCl partial pressure.

Note also that the use of just four external parameters of the laser enables to obtain a wide variability range for output parameters. As these external parameters are easily accessible, this gives the possibility of computerized control of the laser by properly selecting the external parameters and controlling them electronically. As the type of dependence between these parameters is known, this also permits to stabilize the laser operation.

References

[1] JOHNSON T. H., PALUMBO L. J., HUNTER A. M., IEEE J. Quant. Electron. **15** (1979), 289.
[2] STIELOW G., HAMMER T., BÖTTICHER W., Appl. Phys. B **47** (1988), 333.
[3] OHWA M., OBARA M., J. Appl. Phys. **59** (1986), 32.
[4] ROZENKRANZ H., REBHAN U., MUCKENHEIM W., BASTING D., AUSTIN L., Laser Focus, May (1988), 140.
[5] UJDA Z., POKORA L., STEFAŃSKI M., J. Tech. Phys. **32** (1991), 387.
[6] BARANIK C. U., WASSERMAN C. B., LUKIN A. H., Zh. T. Ph. **44** (1974), 2352.
[7] UJDA Z., POKORA L., J. Tech. Phys. **32** (1991), 399.
[8] UJDA Z., Opt. Commun. **85** (1991), 54.
[9] MIYAZAKI K., HASAMA T., YAMADA K., FUKATSU T., EUVA T., SATO T., J. Appl. Phys. **60** (1986), 2721.
[10] TAYLOR R. S., Appl. Phys. B **41** (1986), 1.

Received February 6, 1992
in revised form September 18, 1992